Int J Clin Exp Med 2017;10(4):6845-6852
www.ijcem.com /ISSN:1940-5901/IJCEM0041400

Original Article

Inhibitory effect of celastrol on cell viability of urinary bladder cancer cell line 5637 cells through JAK2/STAT3 signaling pathway

Limin Xu[1], Denghai Zhang[2], Xinghui Liu[1], Chunxin Yang[3], Ying Wang[2], Fanfan Cao[2]

[1]Department of Clinical Laboratory, [2]Sino-French Cooperative Central Lab, Shanghai Gongli Hospital, The Second Military Medical University, Pudong New Area, Shanghai 200135, China; [3]Department of Pharmacy, Affiliated Zhongshan Hospital of Fudan University, Shanghai, China

Received October 8, 2016; Accepted November 10, 2016; Epub April 15, 2017; Published April 30, 2017

Abstract: Bladder cancer is the most common malignancy of various heterogeneous tumor types which occur in the mucous membrane of urinary bladder. Celastrol is a bioactive natural product with anti-cancer anti-oxygenation and anti-angiogenesis functions. In this study, human bladder cancer cell line 5637 cells were treated with various concentrations of celastrol (0, 1, 2 and 4 μM) and evaluated for cell proliferation, apoptotic rate and cell cycle distribution. CCK8 assay showed inhibited cell proliferation of 5637 cells. Besides, induced cell apoptosis and arrested cell cycle were detected by using flow cytometry. Further, Western blot analysis was conducted to explore possible mechanisms involved. Increased Bax along with decreased Bcl-2 and survivin indicated the induced apoptosis through generated ROS and disturbed MMP in 5637 cells. Nuclear translocation showed declined NF-κB in nucleus, indicating the inactivated NF-κB and inhibited Bcl-2, resulting in the apoptosis of 5637 cells. Decreased expression level of JAK2 and STAT3 indicated the blocked JAK2/STAT3 signaling pathway, corresponding to the induced cell apoptosis and arrested cell cycle. In addition, down-regulated MMP9, VEGF and VEGFR2 suggested the inhibition ability of celastrol in angiogenesis. In conclusion, we demonstrated the inhibitory ability of celastrol in cell viability of human bladder cancer cell line 5637 cells. Our study suggested a promising anti-cancer agent and provided reliable data for *in vivo* study.

Keywords: Bladder cancer, celastrol, 5637 cell, JAK2/STAT3 signaling pathway

Introduction

Bladder cancer is the most common malignancy of various heterogeneous tumor types which occur in the mucous membrane of urinary bladder. Bladder cancer can rise at any age, even in child. Bladder urothelial carcinoma (BUC) includes non-muscular-invasion BUC (NMIBUC) and muscular-invasion BUC (MIBUC) [1]. At the current stage, treatment of NMIBUC is mainly electrocision of bladder tumor with irrigation of bladder. Patients suffered MIBUC usually receives surgery with chemotherapy. However, the recurrence of NMIBUC and low effective rate of chemotherapy (40%-65%, approximately) still remain as an intractable issue [2]. Therefore, a new molecular marker for early diagnosis and treatment in clinic is needed currently.

Celastrol extracted from *Tripterygium wilfordii Hook. f.* is a natural product with various bioactivities [3]. Celastrol is a kind of effective proteasome inhibitors. It was demonstrated to induce cell apoptosis through the inhibition of proteasome activity. Current study indicates its strong anti-oxygenation and anti-angiogenesis, which bestows value on celastrol as a bioactive natural product [4]. Efficacy research of celastrol has achieved in anti-cancer and nervicerebrales [5] mouse. In this study, we explored the anti-cancer effect of celastrol on human bladder cell line 5637 cells and investigated the possible mechanisms involved.

Methods and materials

Cell culture

Human bladder cancer cell line 5637 cells were cultured in RMPI-1640 containing 10% FCS and 1% 100× mycilin. Cells were incubated in 5% CO_2 at 37°C for CCK8 and Western blot assay.

Further, for flow cytometry analysis, cultured 5637 cells were digested and transferred into six-well plates at 3×10^5 cells/well. RMPI-1640 containing different concentrations of celastrol (0 for negative control, 1, 2 and 4 μM) were added into each well, respectively. After the incubation for another 48 h, cultured 5637 cells were formed single cell by 0.25% trypsin and washed by 10% PBS, followed by the centrifugation at 1000 RCF for 5 min. Then cells were prepared for following analysis.

CCK8 assay

Cultured 5637 cells treated with different concentrations of celastrol (0, 0.5, 1, 2, 4 and 6 μM) were mixed with 100 μL serum-free RMPI-1640 containing 10% CCK-8 (Dojindo Biochem) and incubated in 5% CO_2 at 37°C for 1 h. The OD_{450nm} of cell suspension was measured using a spectrophotometer at 0, 6, 12, 24, and 48 h after the treatment of celastrolin order to evaluate the cell viability of 5637 cells.

Flow cytometry analysis

The supernatant of centrifuged cells was discarded and then the cells were incubated with Annexin-V fluorescein isothiocyanate (FITC) apoptosis detection Kit (BD Biosciences) for 10 min at room temperature without light. Cell apoptotic rate was measured and the data was obtained using flow cytometry.

Further, cells were collected and resuspended with dyeing buffer containing 50 μM Dihydroethidium (Wegelasi Biotehnology Co., Ltd). Then ROS was measured by flow cytometry (FACSC alibur, BD Biosciences). On the other hand, collected cells were resuspended at the cell concentration of 1×10^6/ml using dyeing buffer containing 1% Tetramethylrhodamine methyl ester (TMRM, immunochemistry technologies). After the incubation at 37°C for 20 min without light, cells were washed with PBS and measured the MMP by flow cytometry.

In addition, prepared 5637 cells were digested and washed, followed by 70% pre-cooled ethanol for 12 h and RNA was removed by using 1 mg/ml RNaseA. Then cells were stained with propidium iodide (PI) for 10 min and the DNA content was measured using flow cytometry so as to determine the proportion of cells in each stage of cell cycle.

Western blot assay

The cells were seeded at 3×10^5 cells/well in six-well plates and duplicated wells were treated with celastrol at 0 (for negative control), 1, 2 and 4 μM. The expression level of NF-κB p65, JAK2 and STAT3 were measured by using Western bolt assay at 3 h after the incubation, while those of VEGF, VEGFR2, MMP9, Bcl-2, Bax and Survivin were analyzed on 48 h, respectively. Cell lysates were prepared in Mg^{2+} lysis buffer. Total protein concentration in each sample was assayed by the BCA method (thermo, USA). Aliquots (20 mg total protein) of each sample were then loaded on 10% sodium dodecylsulphate (SDS)-polyacrylamide gels and after electrophoresis, the proteins were transferred onto a nitrocellulose blotting membrane (millipore, USA) and immunoblotted with specific antibodies and incubated at 4°C overnight. The membranes were then washed and incubated with horseradish peroxidase conjugated anti-JAK2 (Abcam), p-JAK2 (Abcam), STAT3 (CST), p-STAT3 (Abcam), VEGF (Abcam), VEGFR2 (Abcam), MMP9 (Abcam), surviving (CST), Bcl-2 (Santa), Bax (Santa), NF-κB p65 (Abcam), H3 (CST) and GAPDH (CST) antibodies for 1 h at room temperature and then washed and developed according to enhanced chemiluminescence protocols (ECL, millipore, USA). The films of Western blotting were then scanned by using a Bio-Rad imaging densitometer (ModelGS-700) Tanon-5200 and the densities of the bands were semi-quantified using Quantity One 4.2.1 software. The membranes were incubated with 5% skim milk in TBST for 1 h. Then, they were incubated with rabbit anti-HO-1 (1:500 dilutions) primary antibody overnight at 4°C, followed by incubation with HRP-conjugated anti-rabbit IgG (Beyotime) for 1 h, respectively. Immunoreactive bands were detected using an ECL detection kit, and an LAS-4000mini system (Fujifilm Corporation, Kumamoto, Japan) was used for visualization.

Statistical analysis

Data were expressed as mean ± standard deviation of at least three independent replicates and analyzed using *t*-test. GraphPad Prism 5.0 (San Diego, CA, USA) software was used to perform the analysis of data. Differences were considered significant at values of $P<0.05$.

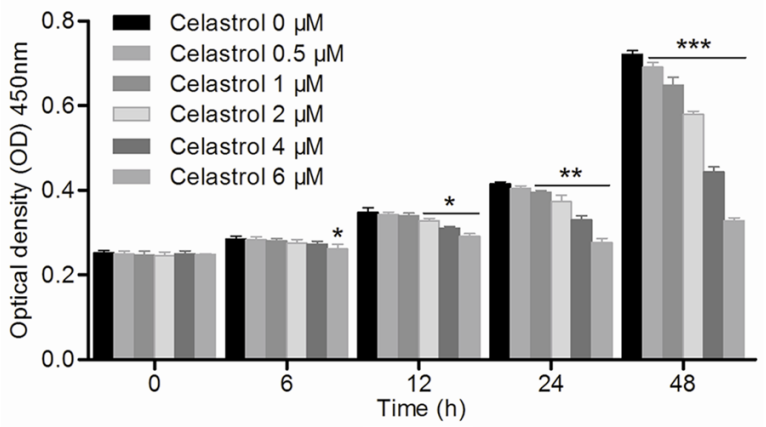

Figure 1. Celastrol inhibits the cell viability of 5637 cells detected by CCK8 assay. The measurement of OD_{450nm} in 5637 cells treated with different concentrations of celastrol indicated the inhibited cell proliferation due to celastrol a time- and dose-dependent manner. *P<0.05, **P<0.01, ***P<0.001, compared to the control group. *n*=3.

Results

Celastrol inhibited cell proliferation

5637 cells treated with celastrol were performed for CCK8 assay to measure the cell viability which was shown in **Figure 1**. As the result, the cell proliferation of 5637 cells treated with 6 μM celastrol presented significant difference at 6, 12, 24, and 48 h (P<0.05 and P<0.001, respectively) compared to the control (0 μM celastrol), indicating that the cell viability of 5637 cells inhibited by celastrol with a time-dependent manner. Besides, 5637 cells treated with various concentrations of celastrol (0.5, 1, 2, 4 and 6 μM) showed declined cell proliferation rate dose-dependently.

Celastrol induced cell apoptosis

Flow cytometry was used to evaluate the cell apoptosis in 5637 cells after the treatment of celastrol (**Figure 2A**). The apoptosis rate was calculated from the percentages of early apoptotic cells presented in the lower right quadrant of the histograms. Significant difference was detected in celastrol groups compared with the control (P<0.05 and P<0.001, respectively, n=3). Compared to the negative control group, the cell apoptotic rate in 5637 cells treated with 1 and 2 μM of celastrol increased significantly (P<0.001, n=3), indicating the induced cell apoptosis by caused by celastrol.

Celastrol arrested cell cycle

The cell cycle distribution of 5637 cells was measured by using flow cytometry. As the result shown in **Figure 2B**, the cell count in each stage was presented visually and the cell circle distribution was calculated. According to the results, the percentage of G2 phase in the celastrol treated 5637 cells dropped significantly from 28.94±1.77% to 19.34±2.81% (P<0.001, n=3) compared with the control group, while that of cells in G1 phase showed an increase from 47.67±2.65% to 62.17±2.45% (P<0.001, n=3), indicating the arrested cell cycle at G1 phase in 5637 cells after the treatment of celastrol.

Generated ROS and disturbed MMP

As shown in **Figure 2C**, the fluorescence intensity of celastrol treated cells was detected much higher than that of controlled cells (P< 0.001, n=3), indicating the high level of ROS content in celastrol treated cells. In addition, declined fluorescence intensity shown in **Figure 2D** indicated the disturbed MMP in celastrol treated 5637 cells (P<0.001, n=3). Generated ROS and disturbed MMP induced cell apoptosis in 5637 cells, according with the result of flow cytometry.

Western blot analysis

As the results shown in **Figure 3A** and **3D**, the expression level of JAK2 and STAT3 decreased dose-dependently with significant difference compared to the control (P<0.001, *n*=3). Angiogenesis related proteins VEGF and VEGFR2 declined with a dose-dependent manner compared to the control group (**Figure 3B** and **3E**, P<0.001, n=3), as well as MMP9 (P<0.001, n=3). Besides, the down-regulated level of Bcl-2 and Survivin, and the up-regulated Bax level corresponded to the result of cell apoptosis analysis (**Figure 3B** and **3E**, P<0.001, n=3). Further, decreased expression level of NF-κB presented significant difference between celastrol treated groups and control (**Figure 3C** and

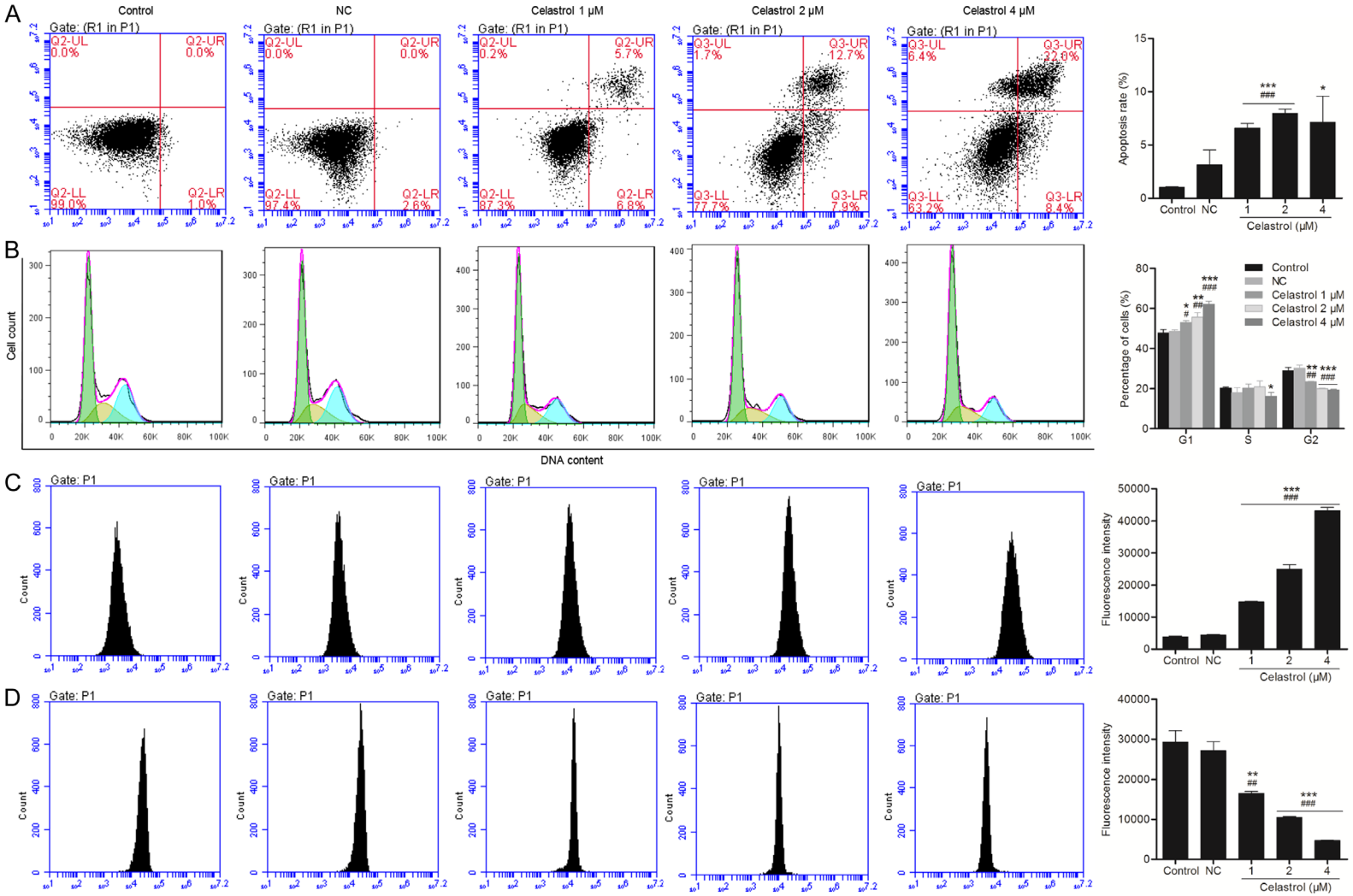

Figure 2. Flow cytometry analysis was performed in 5637 cells to detect cell apoptosis, cell cycle, generated ROS and declined MMP. A. The early apoptotic cells discriminated using Annexin V/PI double staining were shown in the lower right quadrant of the cross coordinates. Cell apoptotic rate of 5637 cells induced by celastrol showed a dose-dependent manner. *P<0.05, ***P<0.001, compared to the control group. $^{\#}$P<0.05, $^{\#\#\#}$P<0.001, compared to the negative control group. *n*=3. B. Cell cycle distribution of 5637 cells was measured by using PI stain assay and flow cytometry after the treatment of celastrol. Increased cells in G1 phase indicated that cell cycle of 5637 cells were arrested in G1 phase dose-dependently. *P<0.05, **P<0.01, ***P<0.001, compared to the control group. $^{\#}$P<0.05, $^{\#\#}$P<0.01, $^{\#\#\#}$P<0.001, compared to the negative control group. *n*=3. C. The fluorescence intensity measured by using Dihydroethidium showed a significant increase in 5637 cells with a dose-dependent manner. ***P<0.001, compared to the control group. $^{\#\#\#}$P<0.001, compared to the negative control group. *n*=3. D. The level of MMP in 5637 cells decreased dose-dependently after the treatment of celastrol. **P<0.01, ***P<0.001, compared to the control group. $^{\#\#}$P<0.01, $^{\#\#\#}$P<0.001, compared to the negative control group. *n*=3.

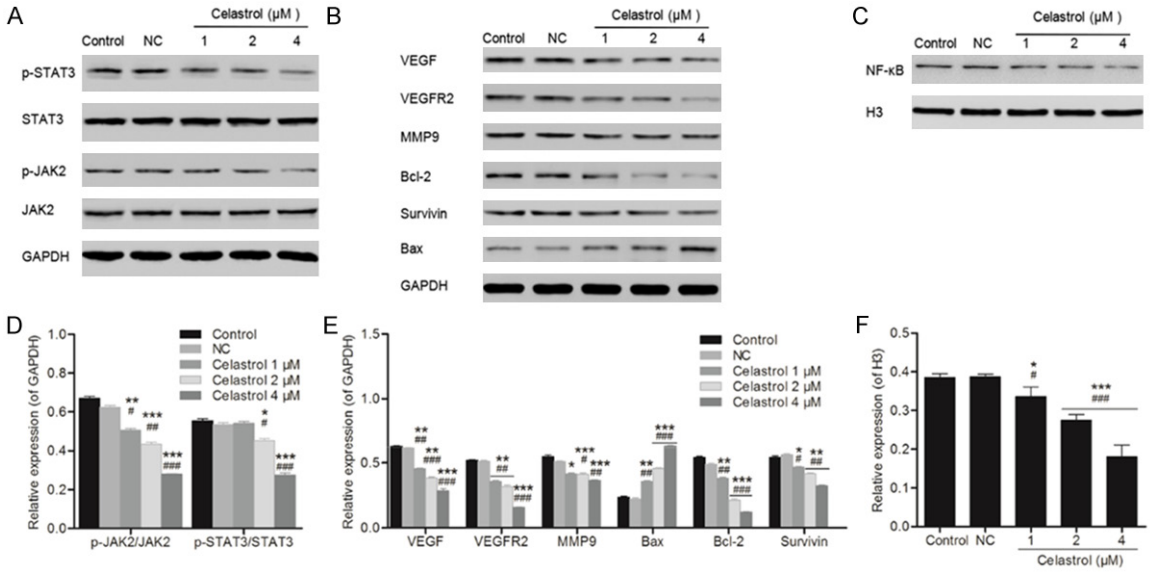

Figure 3. Western blot assay was performed in 5637 cells. A and D. Down-regulated expression level of JAK2 and STAT3 were measured by using western blot after the treatment of celastrol for 3 h. *P<0.05, **P<0.01, ***P<0.001, compared to the control group. #P<0.05, ##P<0.01, ###P<0.001, compared to the negative control group. *n*=3. B and E. Western blot assay was carried out to measure the expression levels of VEGF, VEGFR2, MMP9, Bcl-2, survivin and Bax in 5637 cells after the treatment of celastrol for 24 h. *P<0.05, **P<0.01, ***P<0.001, compared to the control group. #P<0.05, ##P<0.01, ###P<0.001, compared to the negative control group. *n*=3. C and F. Expression level of NF-κB was measured to evaluate nuclear translocation. *P<0.05, **P<0.01, compared to the control group. ##P<0.01, ###P<0.001, compared to the negative control group. *n*=3.

3F, P<0.001, *n*=3), as well as negative control (P<0.001, *n*=3). Inactivated NF-κB led to the declined Bcl-2, resulting in the induced cell apoptosis.

Discussion

Current studies suggested that natural products harbor promising potential in the treatment of various disease and cancer. Celastrol extracted from *Tripterygium wilfordii Hook. f.* is a natural product with various bioactivities. Celastrol is a kind of effective proteasome inhibitors which was demonstrated to induce cell apoptosis through the inhibition of proteasome activity [5] mouse. Current study indicates its strong anti-oxygenation and anti-angiogenesis, which bestows value on celastrol as a bioactive natural product [6]. It was reported that celastrol enhances Nrf2 mediated antioxidant enzymes and exhibits anti-fibrotic effect through regulation of collagen production against bleomycin-induced pulmonary fibrosis [7]. Besides, efficacy research of celastrol has achieved in anti-cancer and nervicerebrales [8]. Previous study demonstrated the inhibition effect of celastrol on human cancer cell lines MCF-7 and PC3 through inhibiting inducible miR-223 further reduces viable cells [9]. In this study, we demonstrated that celastrol inhibited cell proliferation, induced cell apoptosis and arrested cell cycle distribution of human urinary bladder cancer cell line 5637 cells through blocked JAK2/STAT3 signaling pathway, revealing the anti-cancer ability of celastrol.

The expression of apoptotic related proteins Bax, Bcl-2 and Survivin measured by Western blot corresponded to the result of cell apoptosis analysis. Both of Bax and Bcl-2 belong to B-cell lymphoma/leukemia-2 family with multiple highly conservative fragments is mainly distributed in the nuclear membrane, endoplasmic reticulum and mitochondria membrane. Bax harbors apoptotic function inducing the release of apoptosis-promoting substance from mitochondria and the activation of anti-apoptotic proteins Bcl-2 [10-12]. The significant increase of Bax and the decrease of Bcl-2 observed in celastrol treated groups indicated the induced cell apoptosis caused by celastrol, while anti-apoptotic protein survivinis a member of apoptosisinhibitors family. The protein molecule has several cellular actions including

inhibiting apoptosis, regulating cell division and promoting angiogenesis. Survivin expresses during embryonic life but not in terminally differentiated adult tissues. The expression of survivin was reported in BUC while not in normal urothelium due to the differential expression of survivin during embryonic life and terminally differentiated tissues [13]. This implicates the protein as a noninvasive tool for early diagnosis of primary BUC and in followup of patients after removal of BUC in diagnosis [14-16]. Besides, it was also recommended as a cancer vaccine which induces the immune system to mount a cancerspecific immune response against tumor cells in therapy [17, 18]. Several studies reported that high expression of survivin is a poor prognostic marker for the urinary bladder due to the cell proliferation of tumor cells. While declined level of survivin suggests inhibited cell proliferation and induced cell apoptosis. In addition, celastrol was reported to inhibit cell proliferation through the accumulation of increased intracellular ROS and disturbed MMP in cancer cells. It enhances the generation of ROS and trigger apoptosis in cancer cells, which corresponded to the results obtained in our study [6, 9]. In addition, nuclear NF-κB was measured by using Western blot in order to evaluate the nuclear translocation of NF-κB. Transcription factor NF-κB and its inhibitor IκB interplay each other results the coverage of nuclear translocation signal. The nuclear translocation of NF-κB relays on the inactivation of IκB through phosphorylation and proteolysis. Interestingly, IκB including nuclear export sequence which can block the NF-κB signaling pathway through negative feedback loop [19, 20]. NF-κB induces the expression of IκB after the nuclear import, followed by the import of new synthetic IκB. It inhibits the combination between NF-κB and DNA and induces the nuclear export of NF-κB. Declined NF-κB accorded to the down-regulated Bcl-2, indicating the receded nuclear translocation and cell viability.

JAK2 is a kind of non-transmembrane form of tyrosine kinase. While signal transducer and transcription activator 3 (STAT3) plays critical role in the signal transduction and transcription activation. JAK2/STAS3 signaling pathway is a signal transduction pathway stimulated by cytokines. It has a function of wide range including proliferation, differentiation, apoptosis, cell cycle and immunoregulation [21-23]. Constitutive activation of JAK2 was reported in childhood T cell acute lymphoblastic leukemia. STAT3 was found constitutive activated in breast carcinoma and non-small cell lung cancer correlated with induced cell proliferation and inhibited cell apoptosis [24] Epidermal Growth Factor. Besides, activated STAT3 led to oncogenesis was demonstrated. Oppositely, suppressed JAK2/STAT3 signaling pathway inhibits cell growth and induces cell apoptosis in various cancer cells. Previous study revealed suppressed cell growth, induced cell apoptosis and arrested cell cycle in colorectal cancer cells due to inhibited JAK2/STAT3 signaling pathway [25]. Further, the study also demonstrated the inhibited cancer cell invasion through the down-regulated downstream proteins MMP9 and VEGF. In our study, declined JAK2 and STAT3 expression level indicated the blocked JAK2/STAS3 signaling pathway in 5637 cells, relating the blocked JAK2/STAS3 signaling pathway with inhibited cell proliferation and induced cell apoptosis, we suggested that celastrol inhibited cell growth of human bladder cancer cell line 5637 cells through inhibited JAK2/STAS3 signaling pathway.

One of the essential conditions for tumor growth is angiogenesis. Tumor angiogenesis factor plays a crucial role in the generation of tumor vessel, the uncontrolled growth of which is an important characteristic of tumor [26]. It was reported that CXCL1 regulates angiogenesis through epidermal growth factor (EGF) and recruitment of tumor associated macrophagocytes (TAMs) *in vitro*. Intensive angiogenesis and over expressed CXCL1 was observed in cornea tissue of rats, while angiogenic response was blocked after the treatment of anti-CXCL1 antibody [27, 28]. TAMs regulated by vascular endothelial growth factor (VEGF), which also known as vascular permeability factor (VPF). VEGF is a kind of specific heparin-binding growth factor in vascular endothelial cells. VEGF, VEGFA and VEGFB were demonstrated to induce angiogenesis through the recruitment of TAMs, which plays an important role in the angiogenesis and growth of tumor cells in gastric cancer [29, 30]. The association of the high expression of VEGF with the metastasis, angiogenesis and survival rate in rectal cancer was also reported. The process of angiogenesis including the proliferation and migration of

endothelial cells, the degradation of basement membrane and the formation of cavity is a complex process regulated by several positive and negative regulatory factors. In addition, tumor metastasis involves epithelial-mesenchymal transition (EMT) and mesenchymal-epithelial transition (MET). MET is accompanied with the degradation of extracelluar matrix (ECM) by matrix metalloproteinase (MMP) family. The basement membrane is important for maintaining tissue organization, providing structural support for cells, and influencing cell signaling and polarity [31]. Degradation of the basement membrane promotes EMT, which is an essential step for the metastatic progression of most cancers. Type IV collagen is the most abundant component of the basement membrane, which is enabled to be degraded by MMP9. As the result obtained in Western blot analysis, down-regulated expression level of VEGF, VEGFR2 and MMP9 suggested the inhibited angiogenesis and metastasis of tumor cells. The results demonstrated the inhibition effect of celastrol on tumor formation of 5637 cells and provided relevant data for *in vivo* study incelastrol against bladder cancer.

In conclusion, we demonstrated that celastrol inhibited cell proliferation, induced cell apoptosis and arrested cell cycle distribution of human urinary bladder cancer cell line 5637 cells through blocked JAK2/STAT3 signaling pathway. We revealed the anti-cancer ability of celastrol in human bladder cancer cells and provided novel evidence of JAK2/STAT3 signaling pathway as a new target for the treatment of bladder cancer.

Acknowledgements

Academic leaders Program of Pudong Health Bureau of Shanghai (PWRd2014-02). The National Natural Science Foundation of China (No. 81400793). Shanghai health and family planning commission General Program (2015-40395). Shanghai Sailing Program (15YF1410-800).

Disclosure of conflict of interest

None.

Address correspondence to: Drs. Fanfan Cao and Ying Wang, Sino-French Cooperative Central Lab, Shanghai Gongli Hospital, The Second Military Medical University, Pudong New Area, 219 Miaopu RD, Shanghai 200135, China. E-mail: yffs.c@163.com (FFC); ying402407@163.com (YW)

References

[1] Knowles MA. Molecular pathogenesis of bladder cancer. Int J Clin Oncol 2008; 13: 287-297.

[2] Ploeg M, Aben KK and Kiemeney LA. The present and future burden of urinary bladder cancer in the world. World J Urol 2009; 27: 289-293.

[3] Salminen A, Lehtonen M, Paimela T and Kaarniranta K. Celastrol: molecular targets of Thunder God Vine. Biochem Biophys Res Commun 2010; 394: 439-442.

[4] Kannaiyan R, Shanmugam MK and Sethi G. Molecular targets of celastrol derived from Thunder of God Vine: potential role in the treatment of inflammatory disorders and cancer. Cancer Lett 2011; 303: 9-20.

[5] Dai Y, Desano J, Tang W, Meng X, Meng Y, Burstein E, Lawrence TS and Xu L. Natural proteasome inhibitor celastrol suppresses androgen-independent prostate cancer progression by modulating apoptotic proteins and NF-kappaB. PLoS One 2010; 5: e14153.

[6] Jang SY, Jang SW and Ko J. Celastrol inhibits the growth of estrogen positive human breast cancer cells through modulation of estrogen receptor alpha. Cancer Lett 2011; 300: 57-65.

[7] Divya T, Dineshbabu V, Soumyakrishnan S, Sureshkumar A and Sudhandiran G. Celastrol enhances Nrf2 mediated antioxidant enzymes and exhibits anti-fibrotic effect through regulation of collagen production against bleomycin-induced pulmonary fibrosis. Chem Biol Interact 2016; 52-62.

[8] Yang HS, Kim JY, Lee JH, Lee BW, Park KH, Shim KH, Lee MK and Seo KI. Celastrol isolated from Tripterygium regelii induces apoptosis through both caspase-dependent and -independent pathways in human breast cancer cells. Food Chem Toxicol 2011; 49: 527-532.

[9] Yadav VR, Sung B, Prasad S, Kannappan R, Cho SG, Liu M, Chaturvedi MM and Aggarwal BB. Celastrol suppresses invasion of colon and pancreatic cancer cells through the downregulation of expression of CXCR4 chemokine receptor. J Mol Med (Berl) 2010; 88: 1243-1253.

[10] Hsu YT, Wolter KG and Youle RJ. Cytosol-to-membrane redistribution of Bax and Bcl-X(L) during apoptosis. Proc Natl Acad Sci U S A 1997; 94: 3668-3672.

[11] Kirkin V, Joos S and Zornig M. The role of Bcl-2 family members in tumorigenesis. Biochim Biophys Acta 2004; 1644: 229-249.

[12] Nechushtan A, Smith CL, Hsu YT and Youle RJ. Conformation of the Bax C-terminus regulates

subcellular location and cell death. EMBO J 1999; 18: 2330-2341.
[13] Makboul R, Refaiy AE, Badary FA, Abdelkawi IF, Merseburger AS and Mohammed RA. Expression of survivin in squamous cell carcinoma and transitional cell carcinoma of the urinary bladder: a comparative immunohistochemical study. Korean J Urol 2015; 56: 31-40.
[14] Altieri DC. Survivin in apoptosis control and cell cycle regulation in cancer. Prog Cell Cycle Res 2003; 447-452.
[15] Chen YB, Tu JJ, Kao J, Zhou XK and Chen YT. Survivin as a useful adjunct marker for the grading of papillary urothelial carcinoma. Arch Pathol Lab Med 2008; 132: 224-231.
[16] Srivastava AK, Singh PK, Srivastava K, Singh D, Dalela D, Rath S, Goel M and Brahma Bhatt ML. Diagnostic role of survivin in urinary bladder cancer. Asian Pac J Cancer Prev 2013; 14: 81-85.
[17] Altieri DC. Targeting survivin in cancer. Cancer Lett 2013; 332: 225-228.
[18] Coumar MS, Tsai FY, Kanwar JR, Sarvagalla S and Cheung CH. Treat cancers by targeting survivin: just a dream or future reality? Cancer Treat Rev 2013; 37: 802-811.
[19] Chandel NS, Trzyna WC, McClintock DS and Schumacker PT. Role of oxidants in NF-kappa B activation and TNF-alpha gene transcription induced by hypoxia and endotoxin. J Immunol 2000; 165: 1013-1021.
[20] Liu B, Sun L, Liu Q, Gong C, Yao Y, Lv X, Lin L, Yao H, Su F, Li D, Zeng M and Song E. A cytoplasmic NF-kappaB interacting long noncoding RNA blocks IkappaB phosphorylation and suppresses breast cancer metastasis. Cancer Cell 2015; 27: 370-381.
[21] Grandis JR, Drenning SD, Zeng Q, Watkins SC, Melhem MF, Endo S, Johnson DE, Huang L, He Y and Kim JD. Constitutive activation of Stat3 signaling abrogates apoptosis in squamous cell carcinogenesis in vivo. Proc Natl Acad Sci U S A 2000; 97: 4227-4232.
[22] Niwa Y, Kanda H, Shikauchi Y, Saiura A, Matsubara K, Kitagawa T, Yamamoto J, Kubo T and Yoshikawa H. Methylation silencing of SOCS-3 promotes cell growth and migration by enhancing JAK/STAT and FAK signalings in human hepatocellular carcinoma. Oncogene 2005; 24: 6406-6417.
[23] Spano JP, Milano G, Rixe C and Fagard R. JAK/STAT signalling pathway in colorectal cancer: a new biological target with therapeutic implications. Eur J Cancer 2006; 42: 2668-2670.
[24] Alvarez JV, Greulich H, Sellers WR, Meyerson M and Frank DA. Signal transducer and activator of transcription 3 is required for the oncogenic effects of non-small-cell lung cancer-associated mutations of the epidermal growth factor receptor. Cancer Res 2006; 66: 3162-3168.
[25] Jorvig JE and Chakraborty A. Zerumbone inhibits growth of hormone refractory prostate cancer cells by inhibiting JAK2/STAT3 pathway and increases paclitaxel sensitivity. Anticancer Drugs 2015; 26: 160-166.
[26] Nyberg P, Salo T and Kalluri R. Tumor microenvironment and angiogenesis. Front Biosci 2008; 1: 6537-6553.
[27] Miyake M, Goodison S, Urquidi V, Gomes Giacoia E and Rosser CJ. Expression of CXCL1 in human endothelial cells induces angiogenesis through the CXCR2 receptor and the ERK1/2 and EGF pathways. Lab Invest 2013; 93: 768-778.
[28] Wang D, Wang H, Brown J, Daikoku T, Ning W, Shi Q, Richmond A, Strieter R, Dey SK and DuBois RN. CXCL1 induced by prostaglandin E2 promotes angiogenesis in colorectal cancer. J Exp Med 2006; 203: 941-951.
[29] Bai Y, Zhu X, Chao J, Zhang Y, Qian C, Li P, Liu D, Han B, Zhao L, Zhang J, Buch S, Teng G, Hu G and Yao H. Pericytes contribute to the disruption of the cerebral endothelial barrier via increasing VEGF expression: implications for stroke. PLoS One 2015; 10: e0124362.
[30] Cui HJ, Yang AL, Zhou HJ, Wang C, Luo JK, Lin Y, Zong YX and Tang T. Buyang huanwu decoction promotes angiogenesis via vascular endothelial growth factor receptor-2 activation through the PI3K/Akt pathway in a mouse model of intracerebral hemorrhage. BMC Complement Altern Med 2015; 28: 91.
[31] Waerner T, Alacakaptan M, Tamir I, Oberauer R, Gal A, Brabletz T, Schreiber M, Jechlinger M and Beug H. ILEI: a cytokine essential for EMT, tumor formation, and late events in metastasis in epithelial cells. Cancer Cell 2006; 10: 227-239.